Detecting and Localizing Space Based Interference on GNSS Signals using Machine Learning

Akshata Patil, R. Eric Phelts, Todd Walter, *Stanford University*

Steffen Thoelert, *German Aerospace Center (DLR)*

Biographies

Akshata Patil is a graduate student in the Department of Aeronautics and Astronautics at Stanford University. She graduated with a Bachelor of Science in Aerospace Engineering from Florida Tech in 2020. Her research interests revolve around enhancing the reliability and security of perception and navigation systems used in autonomous vehicles.

R. Eric Phelts is a research engineer in the Department of Aeronautics and Astronautics at Stanford University. His research involves developing signal monitoring techniques and analysis for SBAS, GBAS, and ARAIM.

Todd Walter is a Professor of Research and director of the GPS laboratory at Stanford University.

Steffen Thoelert: received his diploma degree in electrical engineering with fields of expertise in high-frequency engineering and communications at the University of Magdeburg, Germany. Since then, he has been with the German Aerospace Centre (DLR). Currently he works within the topics of GNSS verification and system calibration.

Abstract

Global Navigation Satellite Systems (GNSS) heavily depend on low-power signals, which operate below the noise floor. This makes them susceptible to interference that can significantly disrupt navigation. Such interference can degrade a receiver's accuracy and reliability in generating Position Navigation and Timing (PNT) solutions and even prevent it from acquiring and tracking nearby GNSS signals. Ground-based interference is relatively easy to identify with a single receiver, its sources can be diverse and widespread. Space-based interference, on the other hand, is difficult to detect without an extensive receiver network, followed by additional complications in identifying its source.

One instance of a space-based interference that began in June 2021 led to the investigation and detection of an unusual power spike in the B3/E6 band, centered at 1268.52 MHz using Trimble's global network of 43 multifrequency receivers. This network is spread across the US and Europe as described in Patil et al., (2023). The interference event, exhibiting a distinct pattern, was confirmed to be space-based due to its simultaneous impact on the entire receiver network for over 24 hours. This paper extends that previous work by further characterizing the interference on B3I, modeling the potential effects of different interferers on various GNSS frequencies, and developing a method for streamlining the process of detecting a space-based interference using machine learning. The goal is to enhance the capability of widely-distributed receiver networks in promptly detecting and attributing the source of interference, aiding in the improvement of GNSS reliability.

1 INTRODUCTION

Uninterrupted operation of GNSS services cannot be guaranteed due to GNSS signals' susceptibility to various forms of disruptions. These systems currently rely on the ability to receive radio frequency signals from over 20,000 km away in space, making them inherently fragile to Radio Frequency Interference (RFI). The impact of interference on these systems cannot be emphasized enough. Signal disruptions hinder GNSS-based technology and services. As a result, there has been a constant battle to continue to protect, toughen and augment these signals to ensure integrity for its users.

With the growing commercial interest in the development of Low Earth Orbit (LEO) satellite constellations, it has become crucial to establish techniques for detecting and localizing space-based interference. Some organizations are specifically designing LEO constellations to cater to the navigation needs of the autonomous vehicles (AV) industry. Interference with these satellites could present significant challenges to those systems. Unlike typical instances of local jamming or spoofing, without coordinated observations taken over a wide area, space-based interference can get challenging to detect.

Detecting space-based interference involves analyzing GNSS data collected worldwide for extended periods and attempting to identify correlations in the interference patterns across multiple global locations. The complexity arises from the need to analyze

GNSS data and correlating the disturbances in signal patterns on a global scale, emphasizing the critical role of innovative techniques in efficiently and accurately attributing this to safeguard the functionality and reliability of GNSS systems.

To meet the rising demand for accurate and reliable GNSS data, Trimble, a leading GNSS service provider, has designed a network of 43 multi frequency receivers deployed across US and Europe as shown in FIGURE 1 below:

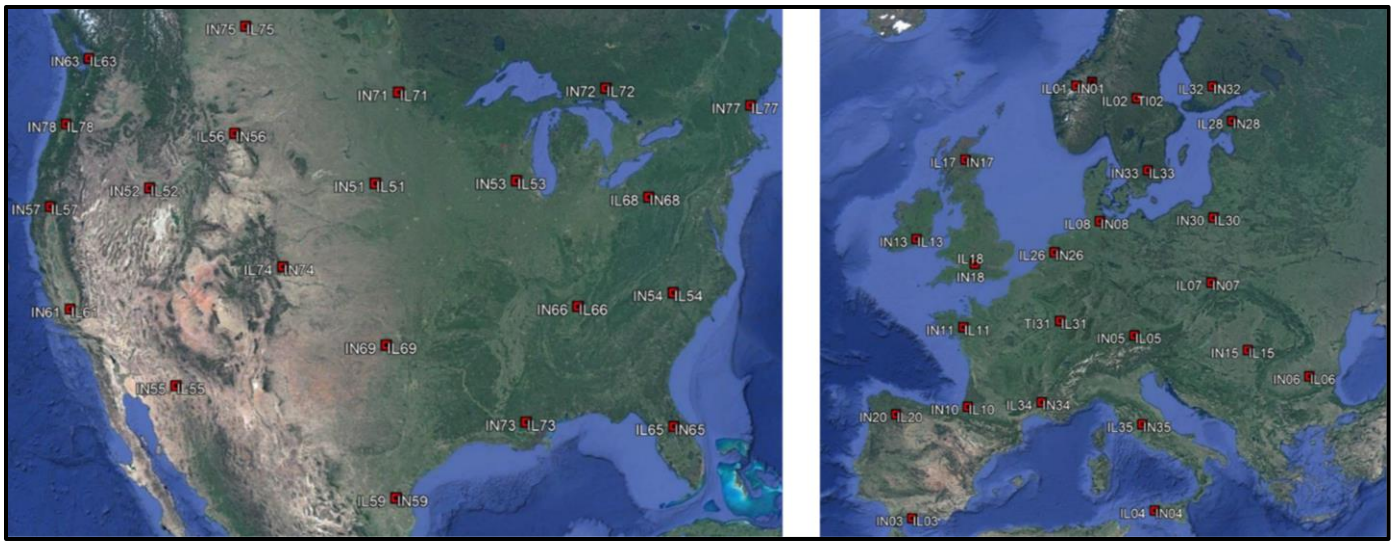

FIGURE 1: Trimble's Receiver Network

Each of these receivers possesses the capability to generate Fast Fourier Transforms (FFT) data taken across multiple frequency bands, averaged over (and output) each minute. This functionality enables users to analyze the mean and standard deviation of signal power across various frequency bands. Leveraging this network of receivers, Trimble initially identified an anomalous spike in signal intensity in the B3-E6 band, specifically centered at Beidou's navigation frequency, B3I: 1268.52 MHz, globally in June 2021. Further investigation revealed that this interference originated from a BDS-3 satellite, BDS-3-M1S, identified globally by the NORAD ID 40749 as described in Patil et al., (2023).

This paper has three main objectives. First, it conducts a further characterization on the previously identified interference on the B3I signal, to offer additional insights into its underlying cause. Second, the paper introduces a machine learning-based method with the aim of expediting the detection of similar space-based interference events in the future. The aim of this method is to improve the effectiveness of current and prospective global receiver networks in promptly identifying and attributing the source of such interferences. Finally, the paper discusses an automation model designed to automatically identify the source of space-based interference detected by the machine learning model.

2 RELATED RESEARCH:

Historically, people have devised a spectrum of spatial (such as Broumandan et al., (2016)) and temporal techniques (Wang, P et al., (2018)) to investigate and address interference, which has been an issue of longstanding concern. Typically, these methodologies involve one or more of the following areas of research per (Ferrara, N. G. et al., 2018):

- Detection: This step involves understanding that there is something wrong with the received signal.
- Localization: This step aims to identify the source of the interference.
- Characterization: This step is focused on examining the interference to understand its root causes and underlying factors.

This paper will discuss a machine learning approach for identifying instances of space-based interference. In addition, it will present an automated algorithm to identify the specific space-based entity responsible for such interference events. The incorporation of advanced models and automated processes is anticipated to improve current state of the art space-based interference detection and localization techniques.

3 APPROACH:

3.1 Characterization:

For further characterization of the space-based interference event originally reported by Patil et. al (2023) on the B3I frequency, researchers at the German Aerospace Center (DLR) captured and analyzed it using a 30 m dish antenna located in Wielheim, Germany. This enhanced analysis yielded the following IQ constellation and spectral flux density as shown in Figure 2 and 3, respectively.

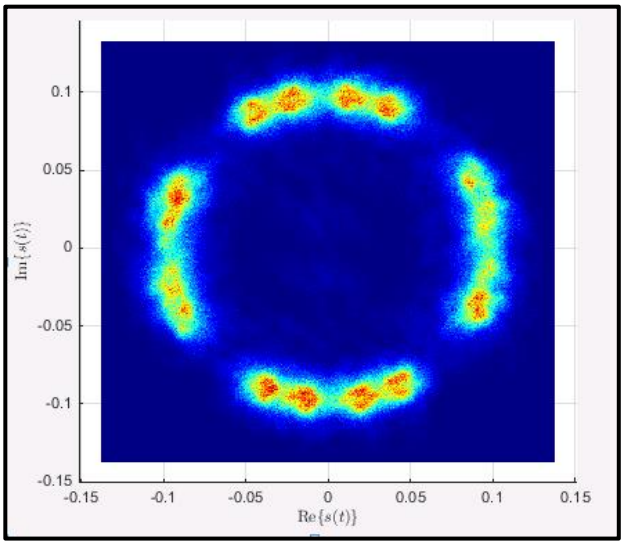

FIGURE 2: IQ constellation of the B3I band

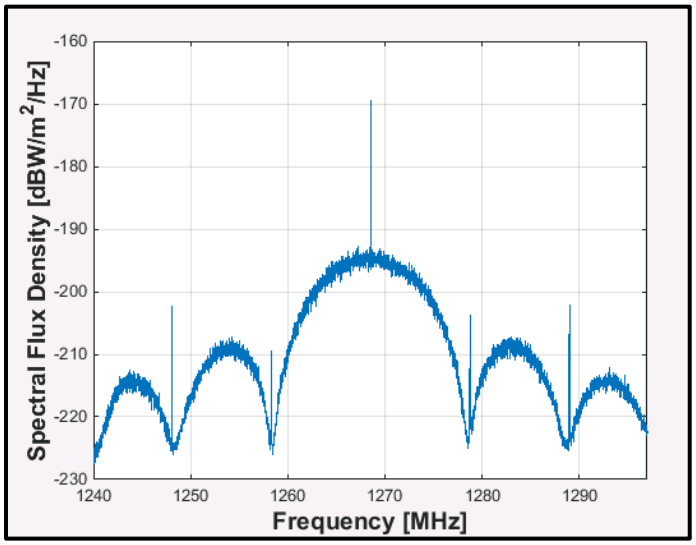

FIGURE 3: Spectra of the B3I band

Upon examining the power spectrum, one can observe the spike centered at the B3I frequency (1268.52 MHz). Additional spikes were also spotted at ± 10 MHz and ±20 MHz from the B3I frequency. These spikes deviate from the anticipated signal spectrum as reported in the Beidou B3I Interface Control Document (ICD).

Further analysis conducted on the real and imaginary part of the B3I signal (as reported in Figure 4) revealed that the spikes in signal intensity appear only for the imaginary part whereas the real part of the signal looks nominal.

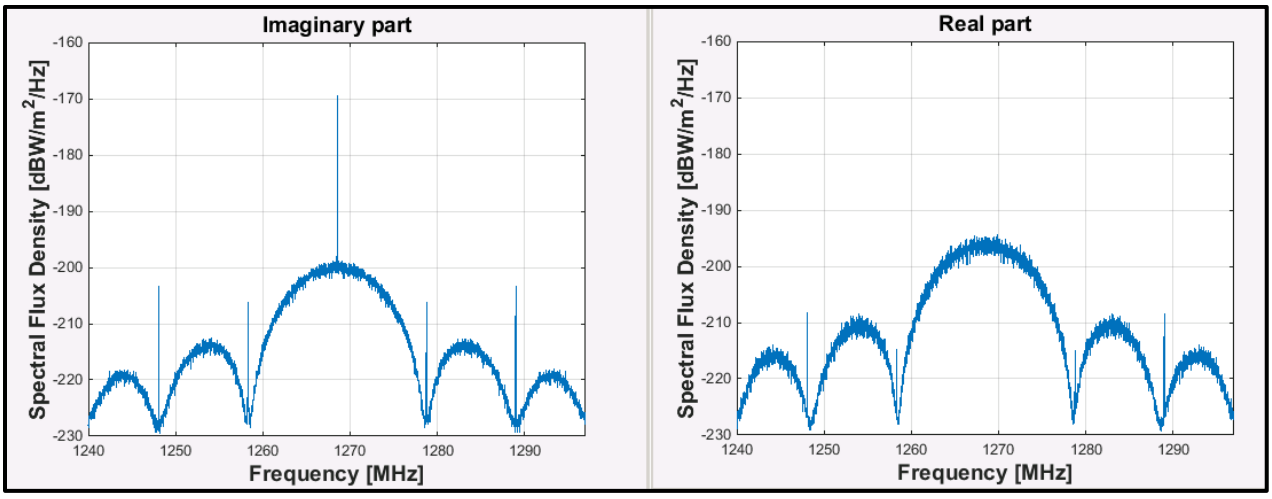

FIGURE 4: Spectral representation of separated imaginary (quadrature component) and real (in-phase) signal component.

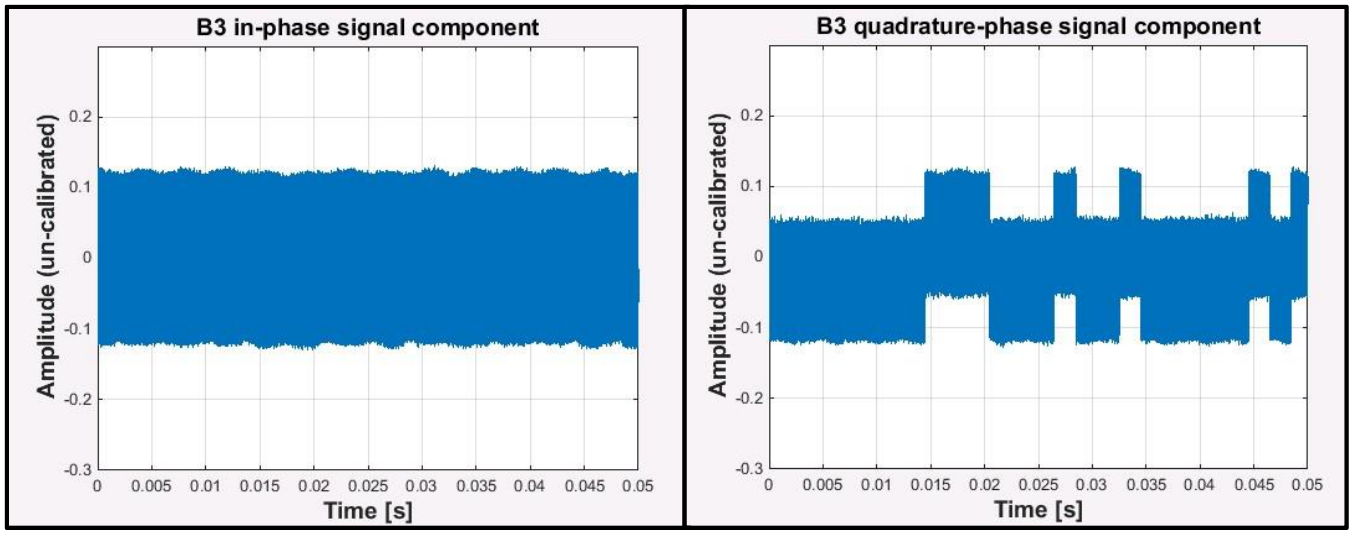

FIGURE 5: Time Series of the I and Q Samples of the B3I signal

Additionally, analysis of in-phase (I-channel) and the quadrature (Q-channel) components (as shown in Figure 5) of the B3I signal revealed that even though the I-channel of the signal appears to be nominal, there is an unexpected overlay on the Q-channel. This is most likely the root cause of the signal spike interference observed on Beidou satellite 40749.

These observations extend the characterization work of Patil, et al (2023) and encourage further investigation into the origin and potential implications of the interference on the BEIDOU-3S M1S satellite.

3.2 Detection:

3.2.1 Challenges:

Detecting space-based interference poses unique challenges as compared to local jamming or spoofing events, primarily because efficiently identifying such interference, requires a widely-distributed network of receivers. The extent of the required network's coverage depends on the orbits of the satellites and the geographical dimensions of the region being monitored. To understand how widespread a network is required to detect a Space Based Interference event, it is crucial to understand the footprint of the satellites presently deployed in Low Earth Orbit (LEO), Medium Earth Orbit (MEO), or Geostationary Earth Orbit (GEO) as shown in Figure 6 below:

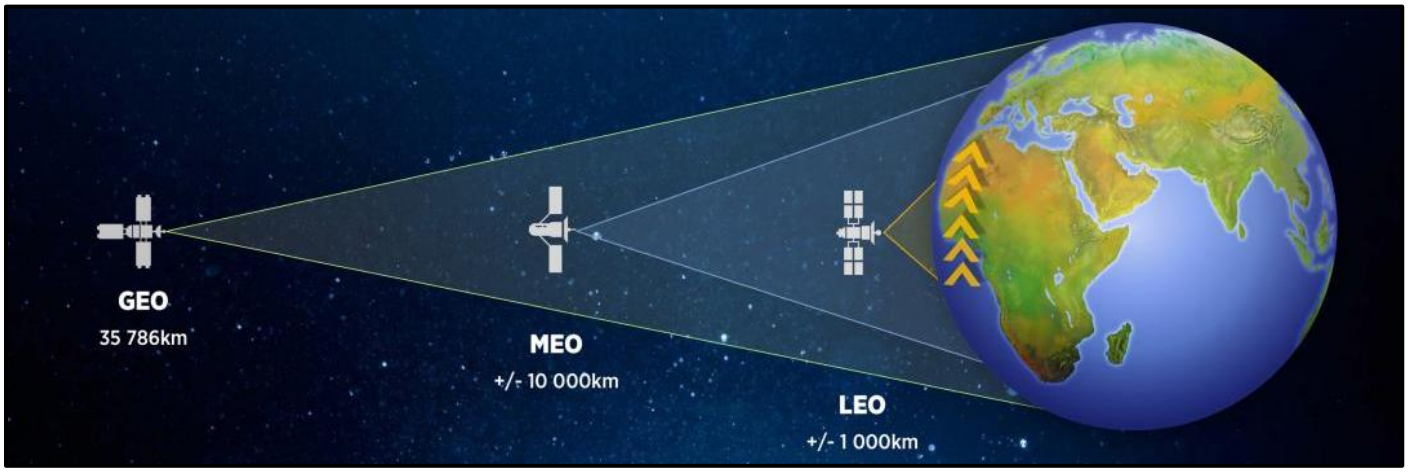

FIGURE 6: Satellite Orbital Analysis [Courtesy of Slingshot Aerospace]

With an elementary orbital analysis for satellites of various orbit altitudes, one can determine the size of the receiver network design. For instance, for efficiently identifying and tracking an interferer originating from LEO, MEO or GEO, a satellite deployed in:

- LEO: has a field of view of 75° and a footprint of 2988 km.
- MEO: has a field of view of 27.16° and a footprint of 8267 km.
- GEO: has a field of view of 17.18° and a footprint of 8968 km.

3.2.2: Real-Time Space Based Interference Detection Techniques:

Since interference can manifest in various forms, such as increased signal power or amplitude, discerning the precise issue with the received signal and determining if the detected fault is consistent across different locations can be a complex task. Questions arise about the correlation of the issue across different locations, its duration, and the specific locations affected. While manually addressing these questions proves challenging, using a machine learning model presents a more efficient means of determining signal interference.

To simplify this manual task, a Support Vector Machine Learning (SVM) model was trained for binary classification, framing the interference detection problem as signal classification—i.e., whether the given signal is interfered or not interfered. In machine learning, binary classification entails learning to distinguish between two categories in a dataset.

Leveraging Trimble's receiver network, daily FFT data (a total of 1440, 1-minute averages for each 24-hour day) was taken from every receiver over each frequency in the B3-E6 band. Then, using the previously discussed Beidou interferer as an archetype, the SVM model was trained to classify which signals from the given frequency band at each location in the network were interfered with (Figure 8) and which were not (Figure 7). For example, using 24-hour FFT data from a ground station located in Sweden, identified by station ID: IN02, the model learned to classify a signal as interfered based on B3I signal monitoring in Sweden.

An alternative method for approaching the modeling of this scenario entails treating it as a computer vision (CV) problem. Detecting interference in a signal requires the continuous examination of hours of data, attempting to discern correlated patterns across various globally deployed stations. Utilizing readily available libraries such as OpenCV for feature extraction through bounding boxes across all signals offers an alternative to address the challenges of identifying space-based interference. However, this approach can be computationally expensive, as it involves processing many images. One would initially need to convert signal information into images, as illustrated below, before inputting them into the model for training. This approach is beyond the scope of this paper.

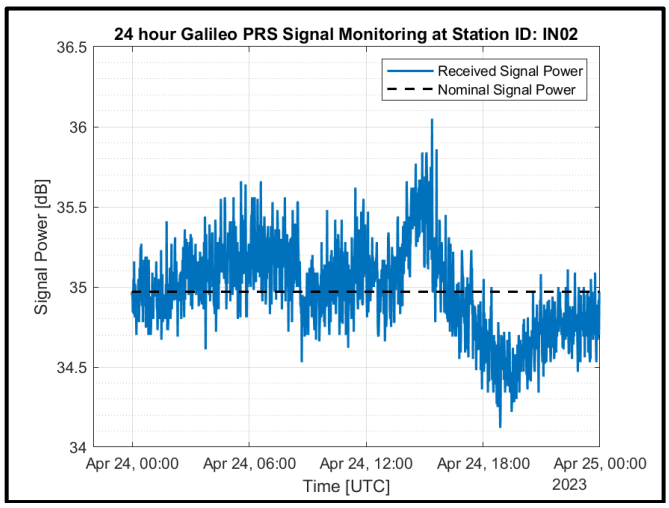

FIGURE 7: Clean Signal

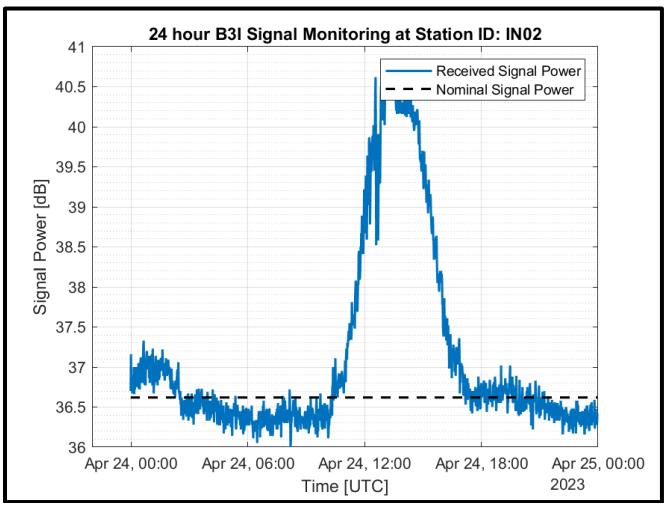

FIGURE 8: Interfered Signal

After training the machine learning model to identify interference, the next step involves monitoring data from multiple stations worldwide. For example, if the model identifies interference in a 24-hour dataset from Sweden, it concurrently observes multiple other locations globally.

For this study, we strategically selected a global network of seven receivers deployed at the following locations:

- Sweden, IN02
- UK, IN17
- South Dakota, IN51
- Arizona, IN55
- Ohio, IN68
- Minnesota, IN71
- New Orleans, IN73

This configuration produces a footprint of approximately 8400 km, providing sufficient coverage to monitor and track interference events originating from Low Earth Orbit (LEO) or Medium Earth Orbit (MEO).

Given that the binary classification SVM model yields either a 1 or a 0 depending on whether the provided 24-hour signal is interfered with or not respectively, a positive interference classification assigns a score of +1 to the respective frequency and respective station. Real-time updates for the simultaneous monitoring of the seven stations get accumulated at the end of a 24-hour period. For instance, for a single day, such as June 27, 2023, if the algorithm generates a cumulative score exceeding 5, the software classifies that specific signal on that day as experiencing space-based interference due to the footprint of the interference.

Presently, this model has been exclusively trained on the space-based interference event reported in Patil et al. (2023). However, it is readily adaptable to training for different types of interference by using datasets containing alternative interference profiles. These steps are outlined in Figure 9 below.

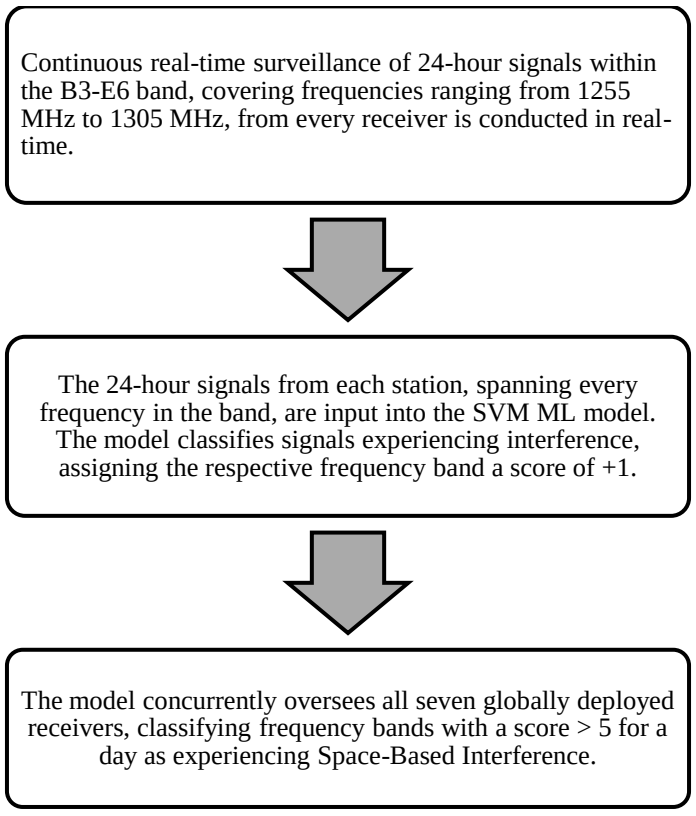

FIGURE 9: Workflow for detecting a Space Based Interference event using the SVM ML Model

3.3 Localization:

Once the detection phase has been completed and the model has identified a space-based interference event for a specific day, the next step is to identify the source of this interference. First, presuming the interferer originates from a satellite, accurate almanac must be used to generate satellite ground tracks. Inaccurate almanac information can cause confusion and misidentification when it comes to correlating the satellite ground track with the interference travelling path.

The approach presented here involves monitoring 24-hour signal FFT data across all frequency bands. Upon detecting a space-based interference event, we compare its ground track pattern over an extended period to confirm whether it originates from low, medium, or geostationary orbits (i.e., LEO, MEO or GEO). For instance, if the interference appears static on receivers only on a single hemisphere of the Earth in over a 24-hour period, it can be confirmed that the source satellite is likely based in GEO. And, according to Roberts, et. al (2023), LEO satellites have an orbital period of 90 to 120 minutes. Therefore, if the interference moves across the globe within such a short period of time, it likely originates from LEO. Lastly, if the interference only appears 1-2 times per day at receivers located around the globe, it likely originates from MEO.

After identifying the source orbit and presuming a candidate constellation within that orbit, each satellite can be monitored within that constellation. In this study, a peak correlation method was used to identify the interference source. This approach entails examining interference events recorded by a station over a 24-hour period. To simplify this, reasonable assumptions can be made to reduce the number of candidate constellations and satellite pass correlations required to analyze for each receiver station. For example, if the interference event occurs at or near a well-known navigation frequency, it is logical to focus on constellations with navigation satellites transmitting that frequency. For example, if the interference event is reported on the B3I frequency, the initial step was to compare interference timestamps with the ground track of all Beidou satellites transmitting the B3I frequency. The same principle applies to L1, L2, L5, E6 signals, and so forth. To illustrate this approach, the B3I interference events on April 27, 2023, are analyzed at four stations from the Trimble receiver network. (See Figures 10 - 13.)

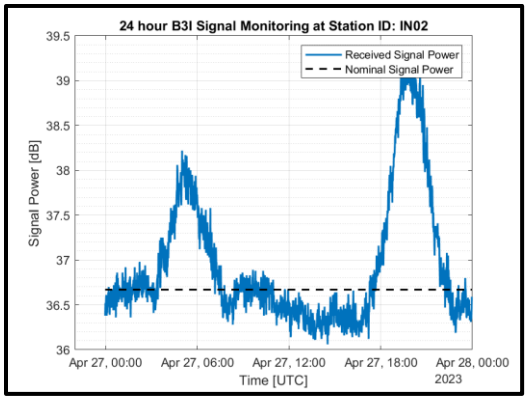

FIGURE 10: Interference Observed in Sweden

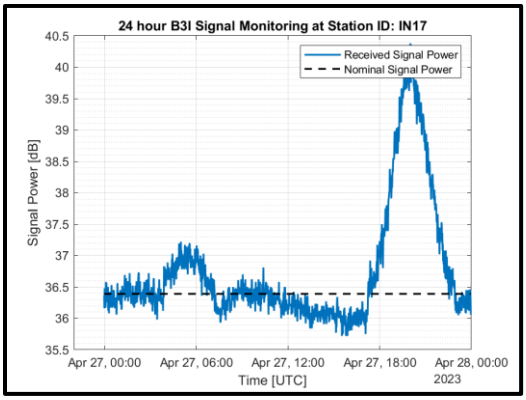

FIGURE 11: Interference Observed in the UK

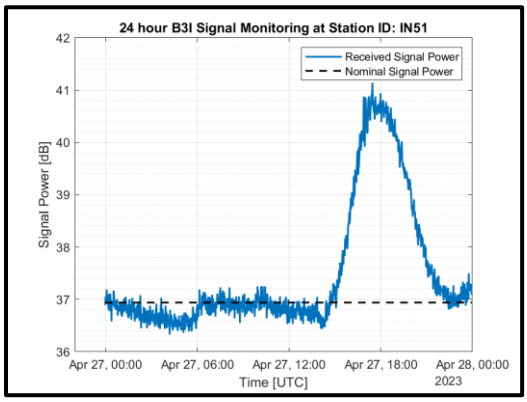

FIGURE 12: Interference Observed in South Dakota

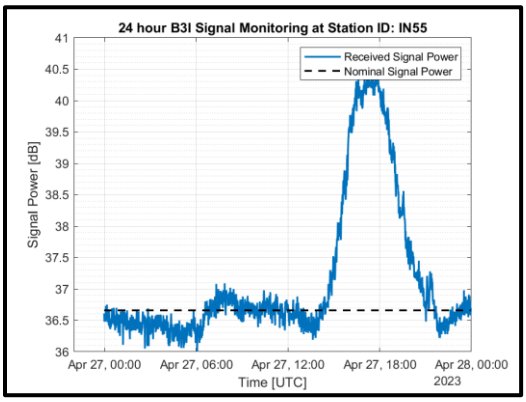

FIGURE 13: Interference Observed in Arizona

Since these events occur at the B3I frequency, the localization process began with a peak-to-peak correlation between the B3I signal power and the ground track of all Beidou3 satellites transmitting the B3I signal. Selecting four Beidou3 satellites (identified by NORAD ID: 40748, 40749, 44864 and 44865), the peak-to-peak correlation method was used.

It's important to note that due to nominal noise and outliers the signal data, a decision was made to apply a smoothing filter. This ensures that the timestamp associated with the peak of the signal power aligns well with the elevation angle profile of the interfering satellite in question. Moreover, to accommodate potential disturbances in the signal data, a margin of +/-5 minutes for the peak was assumed (Figure 16). This allows for margin in case of small peak estimate variations, enabling more accurate identification of the interference source.

The methodology asserts that the peak of the signal power should align closely with the peak of the satellite elevation angle, as illustrated in the subsequent Figures 14 and 15 below. It considers the basic peak correlation strategy but also incorporates signal smoothening and margin for peak-estimation error to enhance the reliability of interference source identification.

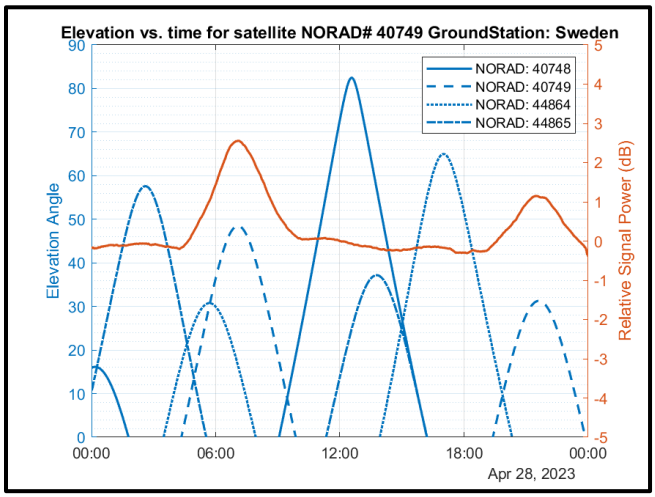

FIGURE 14: Peak to Peak Correlation captured in Sweden.

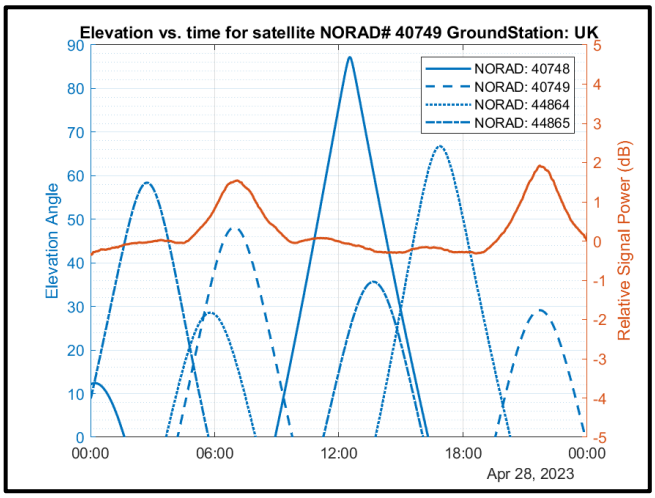

FIGURE 15: Peak to Peak Correlation captured in UK.

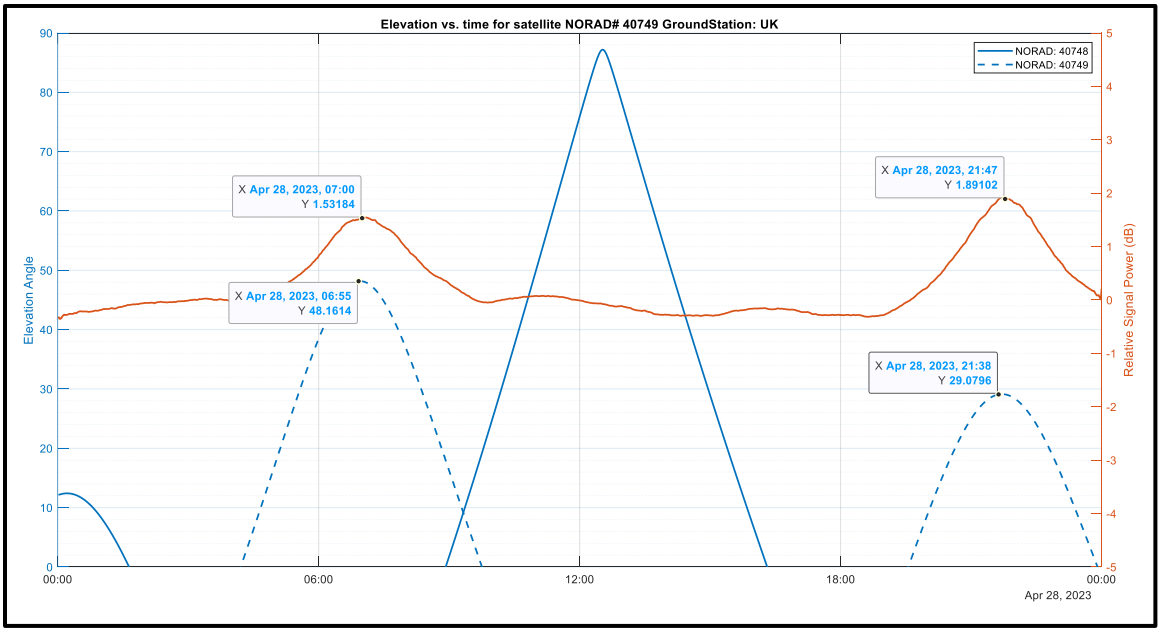

FIGURE 16: Peak estimation with margin to account for small mis-alignments due to noise

4 RESULTS:

4.1 Detection

The machine learning SVM model was initialized and trained to learn whether a given signal was subjected to interference or not. The training dataset spanned multiple timeframes: from the months of June 2021, when the B3I interference was initially identified by Patil et al. (2023), June 2022 and June 2023. This broad temporal window allowed the model to learn the evolving behavior of interference of this type from the initial phase of detection (June 2021) to the most recent data in 2023. In addition, the training dataset was extracted from Trimble's network of 43 multifrequency receivers deployed across the continents of Europe and America. Each receiver captured the entire B3-E6 band, covering frequencies from 1255 MHz to 1305 MHz. This served as the training data for the model's interference detection capabilities.

To validate the model and assess its training effectiveness, a set of 192 randomly chosen GNSS signals, including clean, interfered, and simulated interference cases, underwent testing. The SVM identified the interfered signal in all cases, as illustrated in the confusion matrix below. This underscores the SVM model's ability to successfully distinguish between interfered and non-interfered signals under comparable conditions.

Table 1: Confusion Matrix for SVM Binary Classification Model

		Predicted	
		Negative	Positive
Actual	Negative	120	0
	Positive	0	72

Further, utilizing a randomly selected day, June 27, 2022, the model demonstrated its effectiveness by successfully identifying a space-based interference event on the B3I frequency with a score of +7. This suggests it detected interference at the B3I frequency at all 7 ground stations selected for this test. Future space-based interference of this type could likely be readily detected with such an approach.

4.2 Localization

To assess the accuracy of the localization algorithm, interference was deliberately injected at the same timestamps as satellite 40749 on the Galileo PRS frequency (1278.75 MHz) on a randomly selected day (June 27, 2022). The proposed algorithm was successfully able to identify the responsible satellite. The results from this localization test can be seen in Figure 17 and Figure 18, depicting the PRS signal comparison with satellite 40749's ground track across Sweden and the UK, respectively.

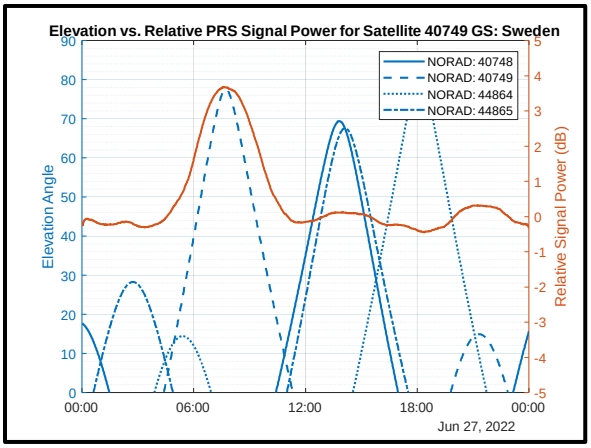

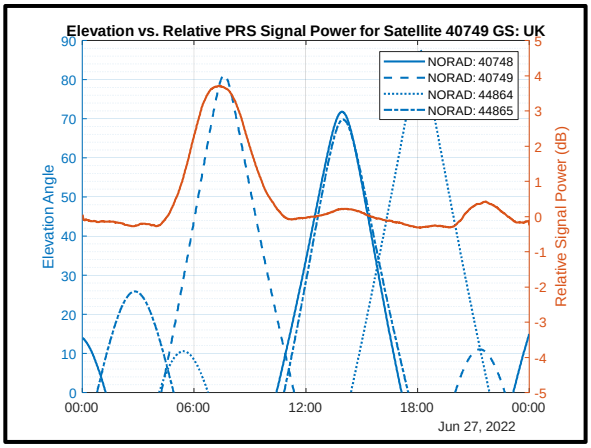

FIGURE 17 and FIGURE 18: Localizing Dummy Interference injected on the Galileo PRS Signal from Sweden and UK

4.3 Simulated Interferer in LEO

To test the algorithm in a very different orbit, a simulated LEO interferer was introduced at a randomly selected frequency of 1300 MHz across our selected network of 7 stations using FFT data from January 16, 2024.

After inputting the simulated data from the network on that day, the SVM model effectively identified a space-based Interference event on January 16, 2024, producing an overall score of +7 for 1300 MHz frequency. The results from detecting this simulated interference are shown in the Figure 19 and Figure 20, which show how ground stations in Sweden and South Dakota captured the interfered signal.

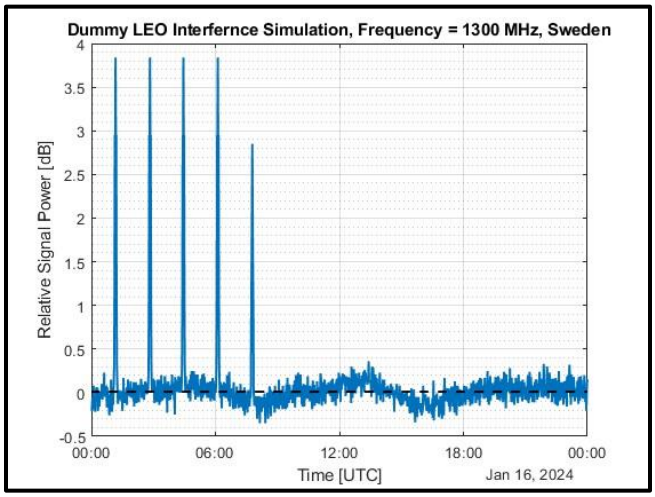

FIGURE 19: LEO Simulated Interference Detection, Sweden

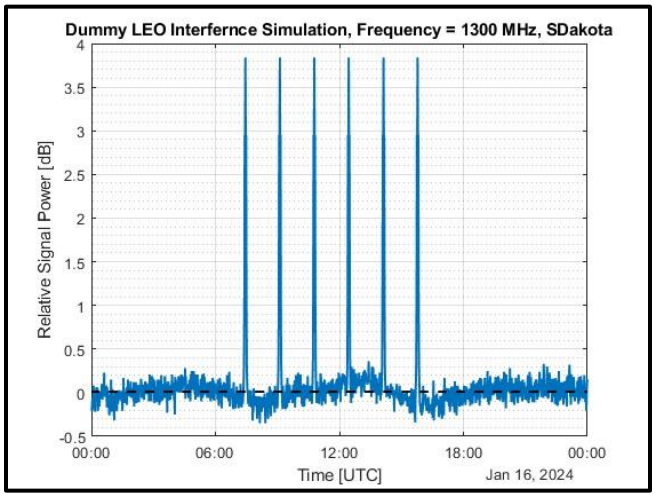

FIGURE 20: LEO Simulated Interference Detection, S. Dakota

Once the space-based interference event was detected by the model, the identification test proceeded to identify the source of the simulated interference using the peak correlation automation algorithm. The localization algorithm was tested using almanac from three LEO constellations – Starlink, Iridium, and Oneweb. The automated localization algorithm was successfully able to detect that the simulated interference originated from the Starlink constellation and specifically from satellite Starlink-1007. The results from this automated space-based interference source identification test can be viewed from Figure 21:

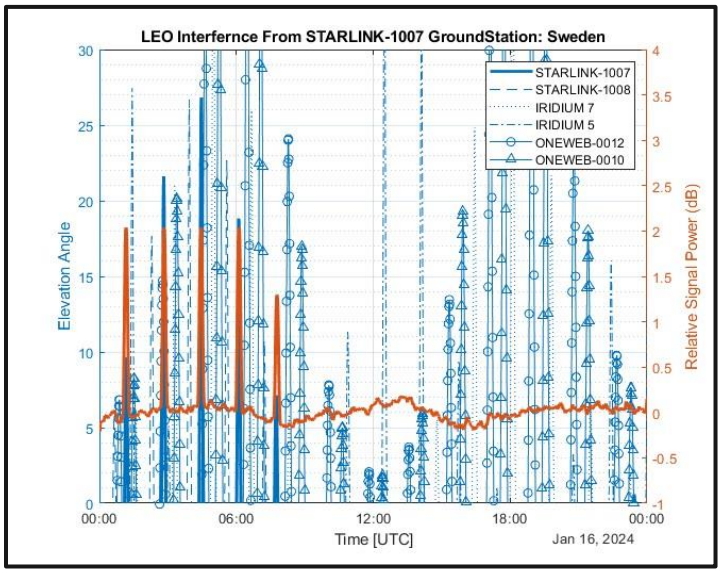

FIGURE 21: LEO Simulated Interference Source Identification from Sweden

Figures 22 and 23 show how the timestamps of the identified satellite align with the timestamps of simulated interference signal as captured from Sweden and South Dakota, respectively:

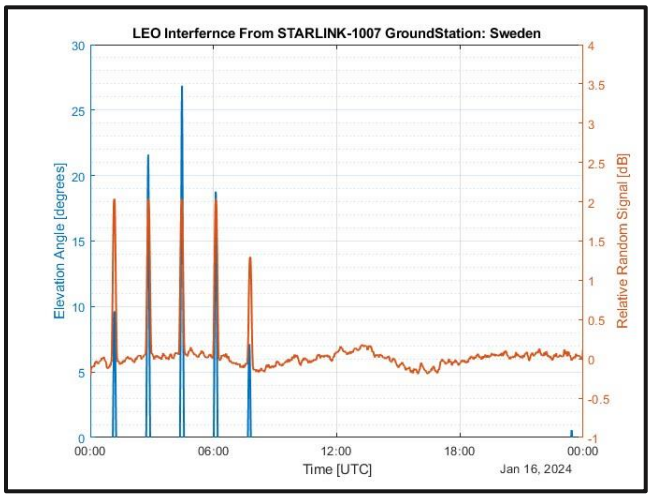

FIGURE 22: Simulated LEO Signal with Starlink- 1007, Sweden

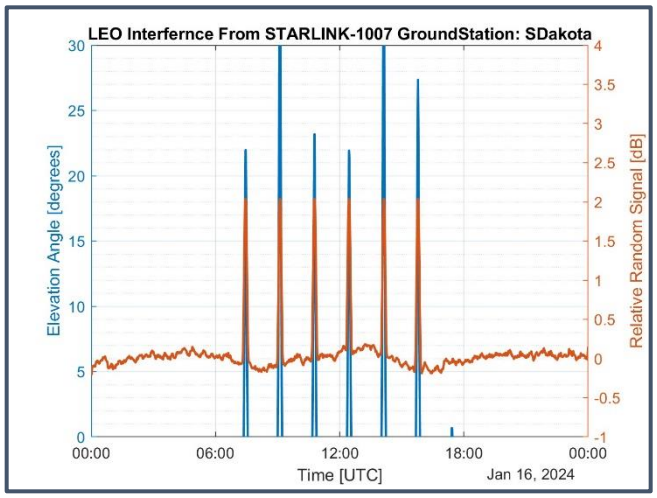

FIGURE 23: Simulated LEO Signal with Starlink- 1007, S. Dakota

4.4 Naturally occurring Space-based Interference

Space-based interference may not always originate from a human made object. A solar flare was detected on the western hemisphere of the globe on December 14, 2023. The event was very short-lived, but, the 24-hour signals from December 14, 2023, were fed into the SVM model to evaluate if it was able to detect any disturbances in the signals. Upon analyzing the FFT data from a receiver in Florida, the SVM model successfully detected disturbances across the entire B3-E6 band on December 14, 2023, by assigning a score of +1 to every frequency in the band. The FFT analysis results from the solar flare test are shown in Figure 24:

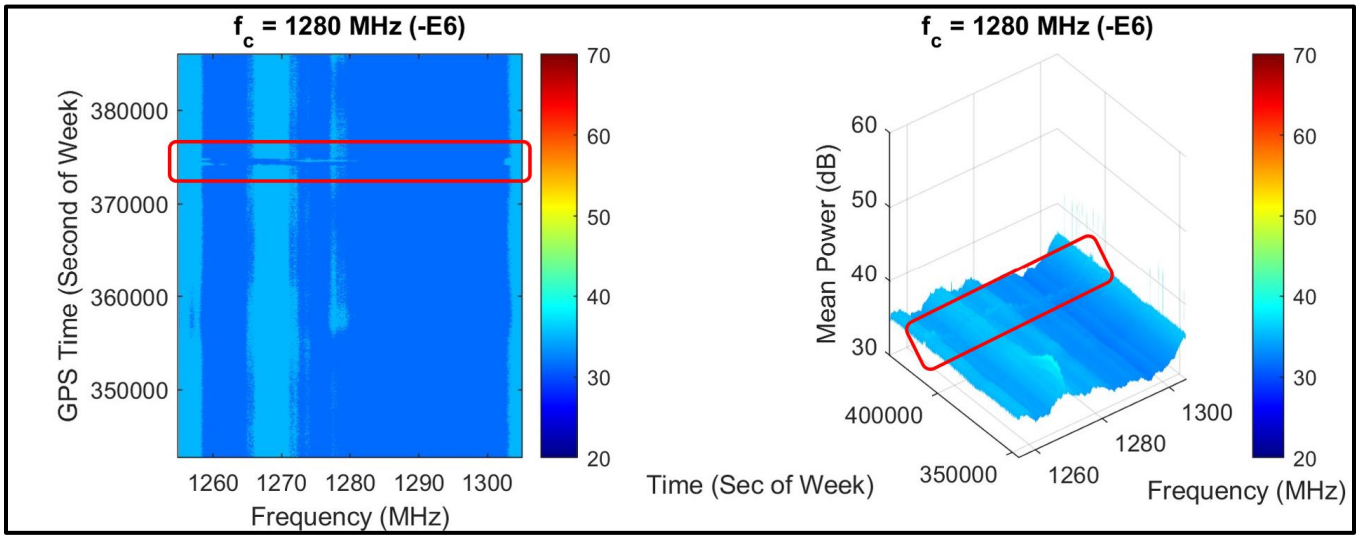

FIGURE 24: FFT Analysis of the Solar Flare Event captured on December 14, 2023, from a ground station in Florida.

While the SVM model effectively detected this event (for the subset of stations able to observe the event), determining the source of the interference currently falls beyond the scope of the peak correlation automatic interferer identification model. This limitation arises because the model is specifically trained to recognize interference events such as the B3I event reported

in Patil et al. (2023). Automatic detection of a different power profile (e.g., pulsed or time-varying) could pose additional challenges, necessitating further research to address it.

4.5 Limitations:

Given the inherent data-driven nature of Machine Learning, this interference detection model has been exclusively trained to identify interference in GNSS data by recognizing abnormal spikes in relative signal power that do not vary with time. However, it's important to note that interference in GNSS signals can exist in various forms, including anomalies in signal amplitude, frequency variations, and more. This model discussed in this paper is specifically tailored to detect interference by following the observed trend in the B3I signal—specifically, a sustained peak in signal power lasting for several hours at each location.

This targeted training approach limits the model's capacity to identify interference beyond this specific scenario. Future plans involve expanding the model's capabilities to encompass other kinds of potential interference cases in GNSS data. By broadening its training data to cover diverse interference scenarios, the model may be equipped with the ability to detect space-based interference promptly and efficiently. This evolution in training will enhance the model's versatility and ensure a more comprehensive approach to GNSS interference detection.

5 CONCLUSIONS:

In conclusion, our investigations, leveraging Trimble's extensive multifrequency receiver network and a 30 m dish antenna, have resulted in the following:

1. **Advanced Detection of Space-Based Interference on GNSS Signals using Machine Learning:**
   Successful training of the SVM ML model enabled real-time detection of space-based interference events. This was realized through a global network of seven strategically deployed receivers, demonstrating the effectiveness of machine learning techniques in detecting interference on GNSS signals.

2. **Advanced Techniques for Localizing Space-Based Interferers:**
   The peak-to-peak comparison algorithm proved successful in localizing and identifying space-based interferer satellites from potentially several constellations each containing many possible sources. This method demonstrated effectiveness in automatically pinpointing the specific space-based sources of interference.

3. **Characterization of B3I Interference:**
   Examination of interference on the B3I signal caused by satellite 40749 revealed new insights about its characteristics. By examining the I and Q channel information, an unexpected overlay code on the B3I signal's Q channel was observed. This anomaly is suspected to be the primary cause of the observed power spike at its center frequency.

The detection and localization methods discussed may assist in making future space-based interferers easier to detect and identify. And the more detailed characterization of the Beidou B3I interference sheds more light on that anomaly and encourages future investigation into its cause and effects.

6 ACKNOWLEDGEMENTS

The authors would like to thank Stuart Riley and Trimble Inc. for generously lending time, equipment, and other assistance with this investigation, and to the Aerospace Corporation for funding this research effort. The authors also would like to thank the FAA and Dr. T.S. Kelso, Operator of Celestrack.

REFERENCES

Patil, A., Phelts, R. E., Chen, Y. H., Lo, S., & Walter, T. (2023). Detecting Space Based Interference on GNSS Signals. *Proc. of the 36th International Technical Meeting of the Satellite Division of The Institute of Navigation (ION GNSS+ 2023), Denver, CO*, 1232-1244. https://doi.org/10.33012/2023.19239

Roberts, T. & Harrison, T. (2022, June 14). Popular orbits 101. Aerospace Security. https://aerospace.csis.org/aerospace101/earth-orbit

Broumandan, A., Jafarnia-Jahromi, A., Daneshmand, S., & Lachapelle, G. (2016). Overview of Spatial Processing Approaches for GNSS Structural Interference Detection and Mitigation. *Proc. Of the IEEE, vol. 104, no. 6, pp.* 1246-1257. https://doi.org/10.1109/JPROC.2016.2529600

Wang, P., Cetin, E., Dempster, Andrew G., Wang, Y. & Wu, S. (2018). GNSS Interference Detection Using Statistical Analysis in the Time-Frequency Domain. *Proc. Of the IEEE, vol. 54, no. 1, pp.* 416-428. https://doi.org/10.1109/TAES.2017.2760658

Murrian, Matthew J., Narula, Lakshay, Humphreys, Todd E., (2019). Characterizing Terrestrial GNSS Interference from Low Earth Orbit," *Proceedings of the 32nd International Technical Meeting of the Satellite Division of The Institute of Navigation (ION GNSS+ 2019)*, Miami, Florida, September 2019, pp. 3239-3253. https://doi.org/10.33012/2019.17065

Ferrara, N.G., Bhuiyan, M.Z.H., Söderholm, S. (2018). A new implementation of narrowband interference detection, characterization, and mitigation technique for a software defined multi-GNSS receiver. GPS Solut 22, 106 https://doi.org/10.1007/s10291-018-0769-z